Beam Diagnostics of the SPring-8 Storage Ring using Undulator Radiation

(1) Accelerator diagnostics beamline II (BL05SS)

BL05SS has an insertion device light source, two optics hutches, and an experiment hutch. The insertion device (ID05) is of out-vacuum type and designed to be able to fit many kinds of experiments. The mounted pure-permanent magnet array, which is made of the ternary alloy Ne-Fe-B (NEOMAX-44H), is of planar Halbach type with the 51 periods of 76mm long. When the magnet gap is a minimum value of 20mm generating a peak field of 0.82T, the deflection parameter $K$ is a maximum value of 5.8, which leads to a multi-pole wiggler (MPW) radiation produced on the many higher-order harmonics that are useful for electron beam diagnostics. The MPW can emit the total radiation power of 10.4kW when the electron beam current is 100mA. By widening the magnet gap, ID05 as an undulator with small $K$ can be also useful for the experiments requiring the higher spectral photon flux and the lower heat load to avoid the thermal drift of a frontend slit or the monochromator.

The layout of the X-ray transport channel of BL05SS is shown in Fig.1. The front end has a X-slit and a Y-slit to shape the white X-ray beam of the ID05. The optics hutch I has the graphite filters and the metal (aluminum) filters, which have moving mechanisms to adjust the intensities and the spectrum of white X-ray beam. The optics hutch II has a cryogenic double crystal monochromator, which covers the photon energy range of 4 to 38keV by (111) reflection of silicon crystals. Beryllium windows have been installed downstream of the monochromator. We can measure energy spectra, angular spectral fluxes and temporal structures of synchrotron radiation (SR) from ID05 in atmosphere, to develop techniques for the beam diagnostics based on observations of the SR. A transport line of the monochromatic X-ray beam from the optics hutch II to the experiment hutch is now under construction. The commissioning of the transport line to the experiment hutch will start in April 2010.

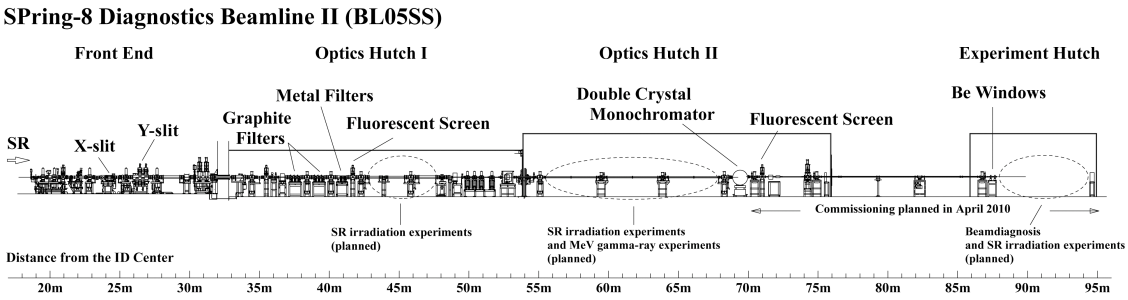


Figure 1: The SPring-8 diagnostics beamline II (BL05SS). The experimental hutch and the SR transport line from the optics hutch II to the experimental hutch will be commissioned in April 2010. Currently, Be windows have been installed downstream of the monochromator in the optics hutch II.

(2) Energy spectrum & Angular spectral flux of ID radiation

The energy spectrum produced by a filament electron beam in a given direction consists of a series of harmonic peaks, the frequency of which are multiples of the fundamental resonant frequency $\omega_1$. For a planar undulator, $\omega_1$ is given by

$$\omega_1 = \frac{2c\gamma^2}{\lambda_u\left(1 + K^2/2 + \gamma^2\theta_x^2 + \gamma^2\theta_y^2\right)} \quad , \qquad \text{eq. (1)}$$

where $\lambda_u$, $K$, $\gamma$, $c$, and $(\theta_x, \theta_y)$ are the period length, the deflection parameter, the electron beam energy divided by $mc^2$, the light speed, and the angle between the electron and the observer, respectively. For a single electron and an observation point, the lobe of on-axis emission is zero for all even harmonics 2, 4, 6, while it reaches a maximum for the odd harmonics 1, 3, 5, the spectrum widths of which are equal to $1/nN$ where $n$ is the harmonic number and $N$ is the number of periods. For a given point of observation, all electrons of a thick beam do not have the same resonant frequency $\omega_1$. This can occur through the angular divergence of the electron beam, which spreads both the horizontal and vertical angles of $(\theta_x, \theta_y)$. A spread of the transverse position of the electron beam also induces a spread of $\omega_1$ because an observer located sufficiently close to the source point sees the radiation emitted by the

various electrons under a different angle ($\theta_x$, $\theta_y$). Equation (1) indicates that the spread in the angle $\theta_x$ and $\theta_y$ shifts the resonant frequency $\omega_1$ to the lower energy side only. As a result, the electron beam emittance leads to the low energy tail of the spectrum through a slit. The energy spread of electron beam also has an effect on a spread of $\omega_1$. If the relative energy spread $\sigma_\gamma/\gamma$ of the electron beam is Gaussian, it introduces a Gaussian spread in the spectrum of each harmonic:

$$\frac{\sigma_\omega}{\omega} = 2\frac{\sigma_\gamma}{\gamma} \quad . \qquad \text{eq. (2)}$$

To be summarized as follows, the peak of the harmonics observed on-axis of the electron beam always has a steep slope on the high energy side which is dominated by $nN$ and by $\sigma_\gamma/\gamma$, and has a reduced slope on the low energy side which is dominated by the emittance, beta function and observation aperture limited by the finite slit width.

The energy spectrum is obtained by measuring the spectral photon flux using an ionization chamber set up in atmosphere, while changing the energy of monochromatic X-ray by scanning Bragg angle of the Si(111) double-crystal monochromator. A rectangular tantalum slit is placed in front of the ionization chamber to measure the on-axis photon flux of ID05. The aperture of the slit was 4.2μrad×4.2μrad. The nominal equilibrium emittance and relative energy spread of 8GeV stored electron beam are 3.4nmrad and $1.1\times10^{-3}$, respectively. A typical example of the energy spectrum of the fundamental harmonic measured at the magnet gap of 80mm, which gives the deflection parameter $K$ of 0.45, is shown in Fig.2. The tail of the low energy side comes from the horizontal emittance. The effect of the slit aperture is negligibly small. The slope on the high energy side is dominated by $1/nN$~0.02. The energy spread has a negligible effect on it. When the magnet gap is the minimum value of 20mm, the deflection parameter $K$ of 5.8 leads to the fundamental harmonic of 0.45keV. As a consequence, many higher-order harmonics are observed in the photon energy range of 4 to 30keV (Fig. 3). For the harmonics higher than the 19th, the energy spread has the non-negligible effect on the slope of the high energy side.

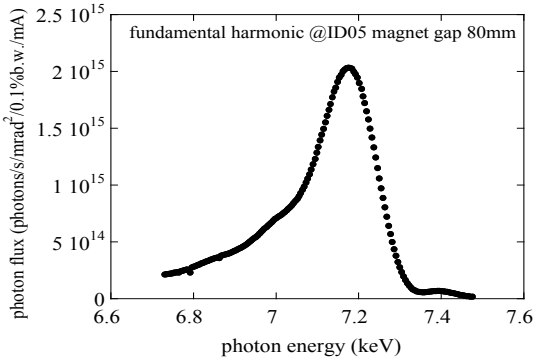


Figure 2: Measured on-axis energy spectrum of the fundamental harmonic when the magnet gap is 80mm. The deflection parameter $K$ is 0.45.

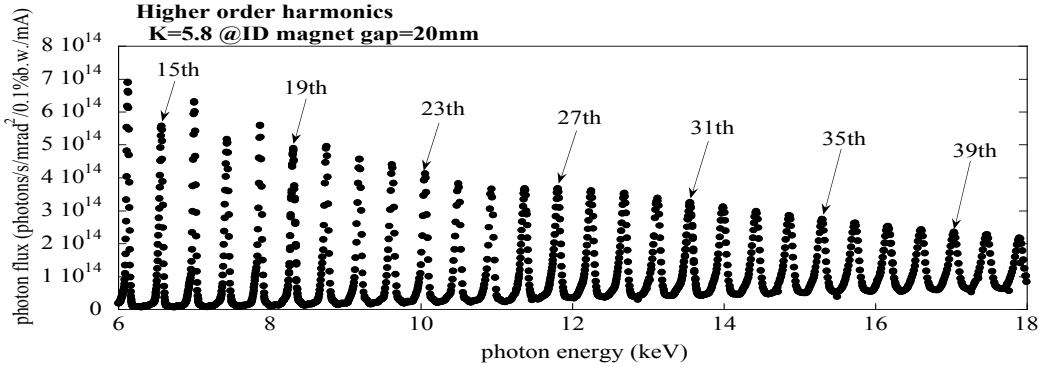


Figure 3: On-axis energy spectrum measured at the minimum magnet gap of 20mm, which gives the deflection parameter $K$ of 5.8. We can see many higher-order harmonics.

Angular spectral photon flux can be also observed using an X-ray CCD camera. Fig. 4 shows an example of the angular spectral flux observed at the photon energy of 8.3keV, which corresponds to

the peak of the 19th harmonic for the magnet gap of 20mm. The center spot is the spatial profile of the 19th harmonic. The outer rings correspond to the off-axis radiations of the 20th and 21th harmonics. The horizontal width of the center spot is determined by the horizontal angular divergence of electron beam, while the vertical width is dominated by the energy spread of electron beam and the intrinsic angular divergence $(\lambda/2L)^{1/2}$ of undulator radiation, where $\lambda$ and $L$ are the wavelength of the radiation and the total length of ID, respectively. The vertical angular divergence of electron beam has a negligible effect due to small emittance coupling ratio.

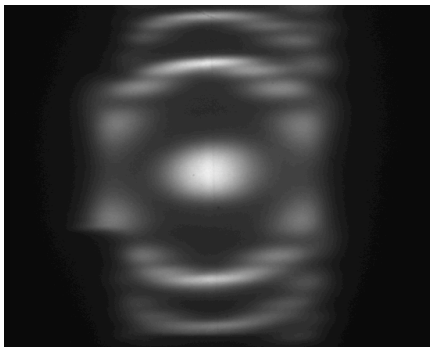

Figure 4: Observed angular spectral flux at the photon energy of 8.3keV corresponding to the peak of the 19th harmonic for the minimum magnet gap of 20mm. The center spot is the 19th harmonic radiation, and two outer rings correspond to the off-axis radiations of the 20th and 21th harmonics.

(3) Observation of the temporal structure using an X-ray streak camera

A streak camera is a device to measure the temporal structure of light pulses. The temporal resolution is typically ~ps. In synchrotron radiation facility, the streak camera is frequently used to measure the SR pulse duration, which reflects the electron bunch length. The principle of operation of a streak camera is illustrated in Fig. 5. The incident light hits a photocathode through a narrow slit aperture. The photocathode converts the incident photon pulses into the photoelectron pulses, which have the same temporal structures as the original photon pulses. After acceleration by an electrode just behind the photocathode, the photoelectrons go through a streak tube in which sweep electrodes are settled. The sweep electrode can rotate the photoelectron bunch transversely, namely, the longitudinal (temporal) structure of the bunch is converted into the transverse profile by the sweep electrode. There are two sweep electrodes (horizontal and vertical) in the streak tube for fast (vertical) and slow (horizontal) sweeps. The vertical fast sweep is applied to measure the temporal structure of each light pulse in consecutive pulse train. The global time structure of the pulse train can be observed by applying the horizontal slow sweep in addition to the fast sweep. After the sweeps, the photoelectrons amplified by a micro channel plate (MCP) hit a phosphor screen at the end of the streak tube. A CCD camera captures the images on the phosphor screen, which corresponds to the time structure of the original photon pulses.

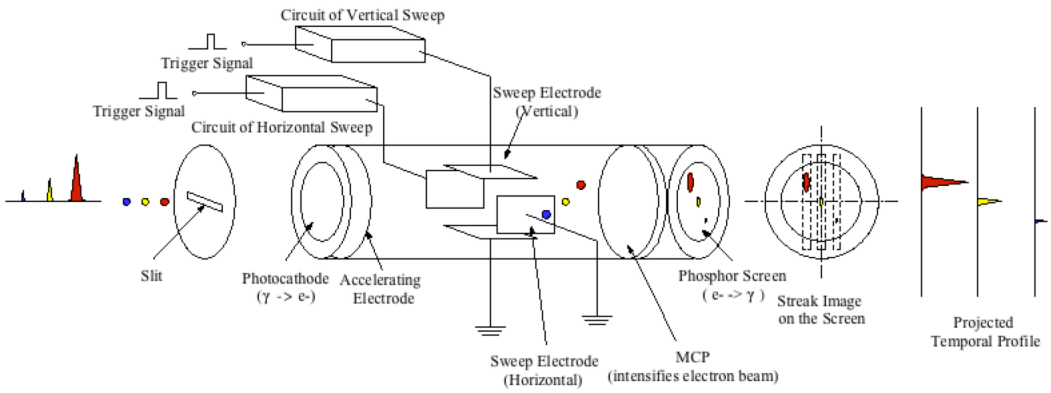


Figure 5: Principle of the streak camera with the dual sweeps by the fast and slow electrodes.